Agricultural Water Management 218 (2019) 94–101

Contents lists available at ScienceDirect

Agricultural Water Management

journal homepage: www.elsevier.com/locate/agwat

Short communication

# Mapping subsurface tile drainage systems with thermal images

Dong Kook Woo[a,b], Homin Song[a], Praveen Kumar[a,c,*]

[a] Department of Civil and Environmental Engineering, University of Illinois at Urbana-Champaign, 205 North Mathews Avenue, Urbana, IL 61801-2352, USA
[b] Now at Lawrence Berkeley National Laboratory, Berkeley, CA 94720, USA
[c] Department of Atmospheric Sciences, University of Illinois at Urbana-Champaign, 105 South Gregory Street, Urbana, IL 61801-3070, USA

ARTICLE INFO

*Keywords:*
Tile drain
Thermal image
Nitrogen loss
Image processing

ABSTRACT

In Midwestern agricultural fields, subsurface tile drainage has been widely used to remove excess water from the soil through perforated tubes installed beneath the ground surface. While it plays an important role in enabling agricultural activities in wet but productive areas, this system is a major driving factor affecting water and nutrient dynamics, and water quality in this region. However, despite its critical role, the specific locations of subsurface tile drainage structures are not generally available nor well captured by conventional optical image processing due to soil surface features, such as topographic depressions and tillage. To overcome these challenges, in this study, we have explored the potential of using thermal images to identify the location of a subsurface drainage pipe. The hypothesis is that the unique spatial distribution of soil moisture set up by tile drains can result in the difference in surface soil temperature between areas near and away from drainage pipes. Toward this objective, we designed and developed an experimental device based on a dimensionless analysis at a scale of 1:20, which was deployed in the open air for 4.5 months. The experimental results demonstrate that (1) there is an ideal time for thermal image acquisition that maximizes the contrast between the regions close to and distant from subsurface drainage systems, and (2) the thermal image processing approach proposed in this study is a promising tool that has advantages of higher accuracy and stability in localizing subsurface drainage pipes over optical image-based approaches

## 1. Introduction

Subsurface tile drainage systems have been widely used for water management technique to remove excess water from the poorly drained soils in the Midwestern United States for more than 100 years (Pavelis, 1987). Approximately 85 percent of croplands in this region have subsurface tile drainage systems (Pavelis, 1987; Sugg, 2007; Jaynes et al., 2010). In general, 0.25 m diameter tile at 1.3 m depth is installed at 20 m spacing although a proper configuration of the tile layout for a given field is highly dependent on soil type, slopes, surface conditions, and crops (Fraser and Fleming, 2001; Wright and Sands, 2001). Tile outlets are generally located at drainage ditches, waterways, streams and/or wetlands. Most crops require specific soil moisture conditions for their growth and do not tolerate and survive well in soils that are constantly wet. Tile drain systems enable earlier planting (Kornecki and Fouss, 2001) and improve soil aeration (Lal and Taylor, 1970; Fausey, 2005). Therefore, high crop yields are attained (Cannell et al., 1979; Du et al., 2005). For example, Helmers et al. (2017) observed a 10 percent increase in average corn yield and a 5 percent increase in average soybean yield, compared to sites without subsurface drainage. Therefore, it is out of great necessity to achieve increases in crop yields in wet but productive areas by avoiding crop mortality due to waterlogging (Zucker and Brown, 1998). Despite the advantages of drainage tile systems, they can also increase nutrient losses through the root zone by channeling subsurface water runoff to tile drainage, which increases riverine nutrient loads and subsequent degradation of receiving water bodies (Fausey et al., 1995; Li et al., 2010; Radcliffe et al., 2015; Woo and Kumar, 2019). To reduce nitrogen loss and increase crop nitrogen use efficiency, the safe drainage time was estimated to be 11–16 days after fertilizer applications (Wang et al., 2011). In addition, Li et al. (2010) showed that approximately 80% of stream water and 90% of nitrate are contributed by tile drain flows in this region. However, the specific locations of tile drainage systems are not generally available (Allred et al., 2018), hindering the spatial analysis and modeling.

There are several studies attempting to identify subsurface drain lines. By employing soil physical properties, land cover, and aerial optical images, Naz and Bowling (2008) conducted a decision tree classification to estimate potential tile-drained areas and then perform

* Corresponding author at: Department of Civil and Environmental Engineering, University of Illinois at Urbana-Champaign, 205 North Mathews Avenue, Urbana, IL 61801-2352, USA.
*E-mail addresses:* dkwoo@lbl.gov (D.K. Woo), hsong36@illinois.edu (H. Song), kumar1@illinois.edu (P. Kumar).

https://doi.org/10.1016/j.agwat.2019.01.031
Received 23 July 2018; Received in revised form 31 December 2018; Accepted 22 January 2019
Available online 27 March 2019
0378-3774/ 

image processing to locate subsurface tile drain pipes. High-resolution color infrared and surface slope data, and directional first differential horizontal and vertical filtering techniques have been also used to improve the detections of tile drain locations (Northcott et al., 1996; Varner et al., 2002; Naz et al., 2009). However, none of these methods are able to attribute surface signatures arising from tile drains as distinct from other surface features, such as topographic depressions and tillage. Such a distinction appears to be essential since the specific tile locations are highly desirable for performing accurate simulations of subsurface water and nutrient processes at fine spatial resolution (~1 m) (e.g. Woo and Kumar (2019)) and for identifying hot spots where the inputs of nutrient are produced in intensively managed agricultural landscape (Randall and Iragavarapu, 1995; Dinnes et al., 2002).

The abovementioned background leads us to a point that the reliable prediction of subsurface tile drains cannot be achieved by using spatial optical images due to the existence of other surface features similar to tile drain lines, such as tillage and machinery traffic (Verma and Cooke, 1996; Naz et al., 2009). To improve its accuracy, we propose the use of thermal images instead. That is, a unique spatial distribution of soil moisture set up by tile drains can result in differences in surface soil temperature between near and distant points from tile drain pipes. This is because a convex subsurface water potential between tile drains subsequent to precipitation (Fig. 1a) provides distinct characteristics of soil heat capacity compared to the period long after precipitation (Fig. 1b). The reduction of moisture above the tile results in a decrease in soil heat capacity near tile drains thereby increasing in surface soil temperature. Therefore, in this study, we posit that the spatial variations in surface soil temperature resulting from soil moisture variation induced by tile drains are effective indicators to define the locations of subsurface tile drainage pipes.

The overarching objective of this study is to experimentally validate the feasibility of the use of thermal images to map agricultural subsurface drainage systems. Toward this objective, we conducted down-scaled experiments along with thermal image processing to investigate the extent to which using thermal images is a convincing experimental method to detect subsurface tile drains. Therefore, in this study, we are not striving to obtain large-scale tile maps but rather to attempt to assess its feasibility by producing comparable macroscopic scale patterns and trends using a simplified experimental design.

## 2. Methods

### 2.1. Experimental design

A down-scaled experimental setup was designed based on the dimensionless study used in Shokri and Bardsley (2014) at a scale of 1:20 as shown in Fig. 1c and d. A perforated plastic drainage pipe was installed in the middle of the experimental domain (1 m long, 0.5 m wide and 0.244 m high) at the depth of 0.067 m in the direction of width. Two drainage outlets are located through the walls. The internal diameter of the pipe was 0.013 m and five rows of $7 \times 10^{-5}\,m^{-2}$ drain holes were drilled at every 0.035 m over the length of the pipe for drainage water to enter. The dimensions used in this study enable dynamics and processes naturally occurring in tile-drained agricultural fields to be reproduced. The dimensions were also designed to meet the specific need of measurement and instrumentation systems: maximizing the area covered by the thermal camera used in this study while

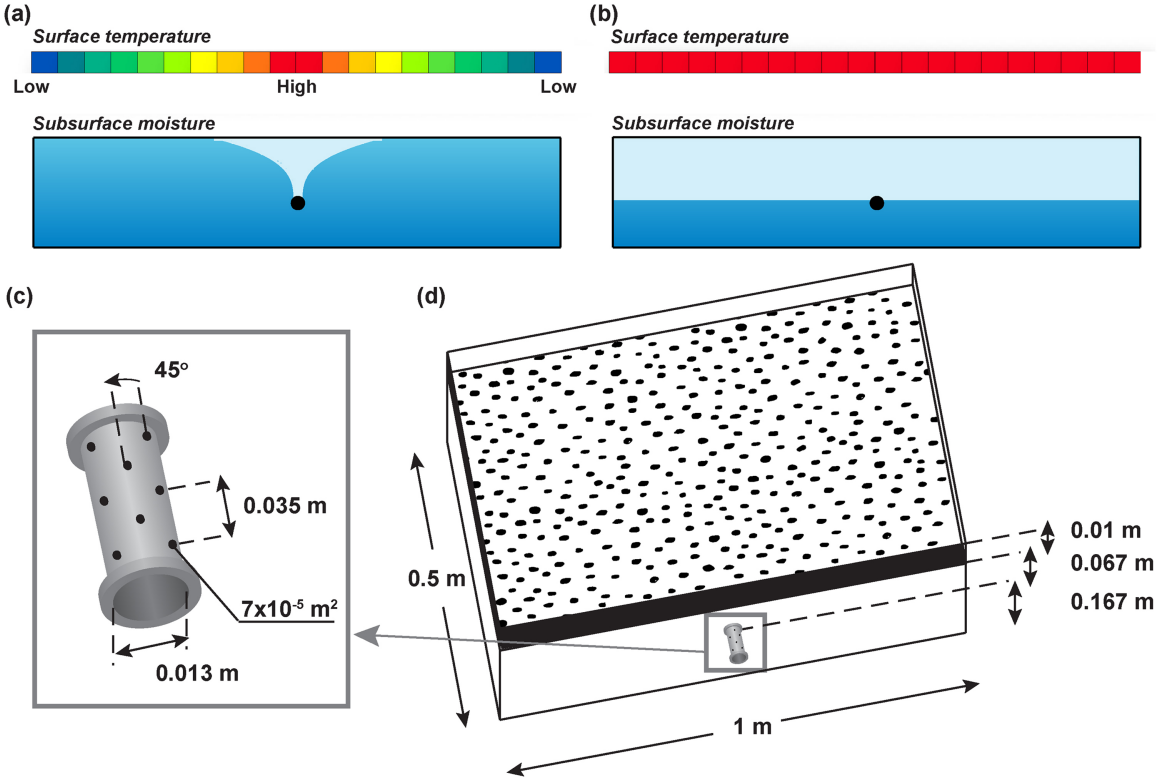


**Fig. 1.** Schematic diagrams of relative surface temperature (top panels) and subsurface water table (bottom panels) in a tile drainage system (a) a few days after and (b) long after precipitation events. The black circles in the bottom panels show the location of tile drain. Due to subsurface water table gradients toward a drainage tile, soil moisture should be relatively lower in the area near the tile drain than the other. The reduced soil moisture results in decreasing soil heat capacity thereby increasing soil temperature. In this study, we use (c) a perforated plastic drainage pipe that is installed in (d) an experimental equipment designed based on a dimensionless domain used in Shokri and Bardsley (2014) at a scale of 1:20.

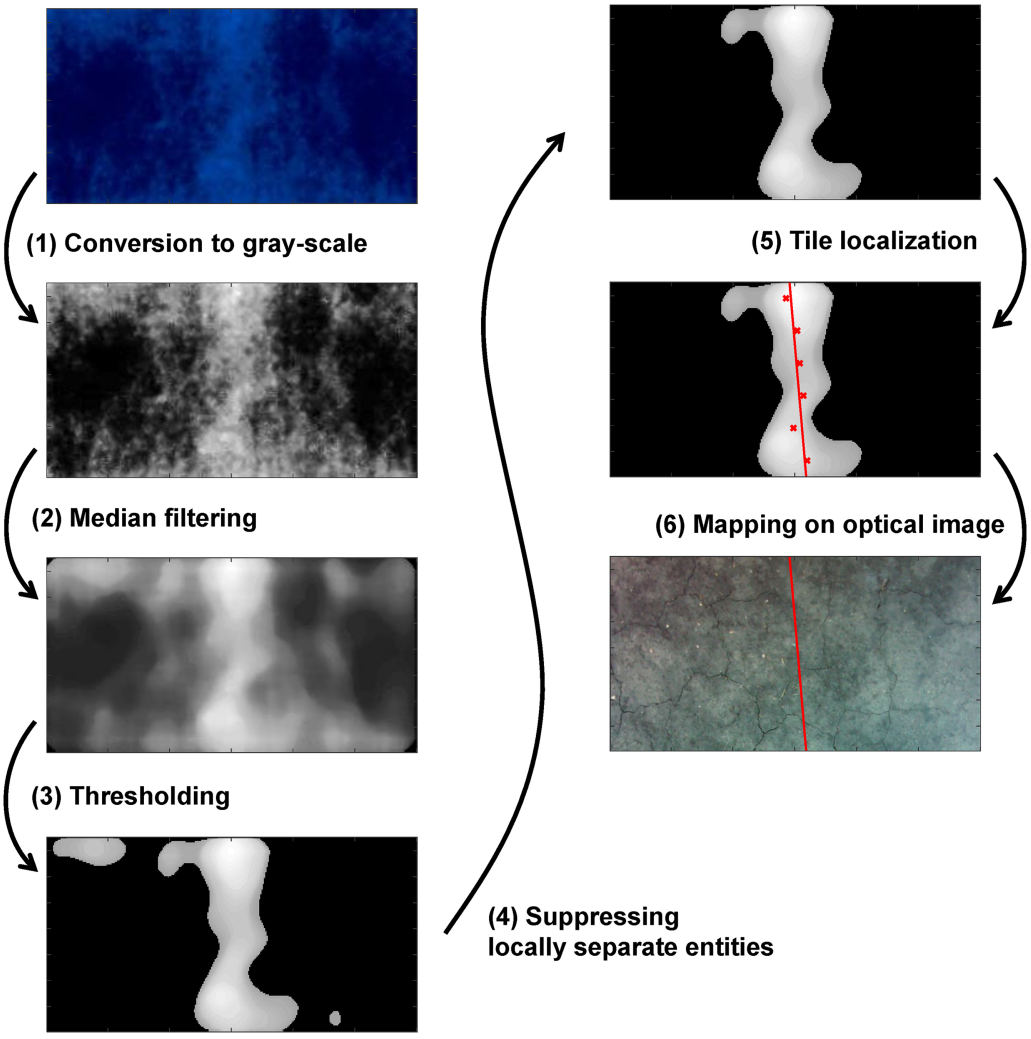


**Fig. 2.** An overview of the proposed tile detection algorithm.

minimizing blurring effects caused by the thermal camera.

An infrared camera (T620, FLIR Inc.), featuring the temperature resolution of 0.04 °C, was used to obtain surface thermal images. For reference, optical images were also acquired using the optical camera integrated with the infrared camera while thermal images were taken. To create a soil environment similar to the agriculture field, soils were collected from an agricultural field (Latitude: 40.03 and Longitude: −88.66) in September 2017, which supported corn-soybean rotation. The soils were characterized as a mixture of Ipava silt loam and Sable silty clay loam that had relatively low hydraulic conductivity (e.g. the typical range of saturated hydraulic conductivity is from 1.08 cm $d^{-1}$ to 1.68 cm $d^{-1}$ (Carsel and Parrish, 1988)) with granular structure as a typical soil property in this area (Wilkins et al., 2019). The soil sample was exposed to the natural environment so that soil surface energy dynamics with subsurface tile drainage systems can interact with natural weather conditions.

The experiments were conducted from October 1, 2017 to February 15, 2018. This testing period correspond to the non-growing period that helps minimizing the error caused by a thick vegetation cover. To allow time for the suppression of transients from the experimental setup due to disturbed soil conditions, the experimental equipment was left deployed for a month and then we started obtaining thermal images. Thermal and optical images were taken to fully cover the surface of the experimental device and obtained around noon when the solar radiation was strong enough to heat up the surface and hence to enhance the contrast between the areas close to and distant from the subsurface drainage pipe within the sample surface. Although the thermal image collection was performed regularly throughout the testing period, a strict daily-based collection was not available mainly due to intermittent unfavorable weather conditions (e.g. snows and heavy rains).

### 2.2. Tile detection algorithm

To improve the accuracy of tile drain recognition, we performed image processing on the thermal images. Also, the study domain was reduced by 20% on each side for the image analysis to minimize boundary effects within the experimental device. An overview of the developed tile detection algorithm is provided in Fig. 2. First, a raw thermal image represented in the RGB colormap was converted into a gray-scale image. Then, denoising operation was performed by two-dimensional (2-D) median filtering to remove salt and paper-like noise in the gray-scale image (Acharya and Ray, 2005). The denoised image by the median filtering, $T_{med}(m, n)$ where $m$ and $n$ denote image dimension, is given by

$$T_{\text{med}}(m, n) = \text{median}\{T(m - k, n - l), (k, l) \in W\} \quad (1)$$

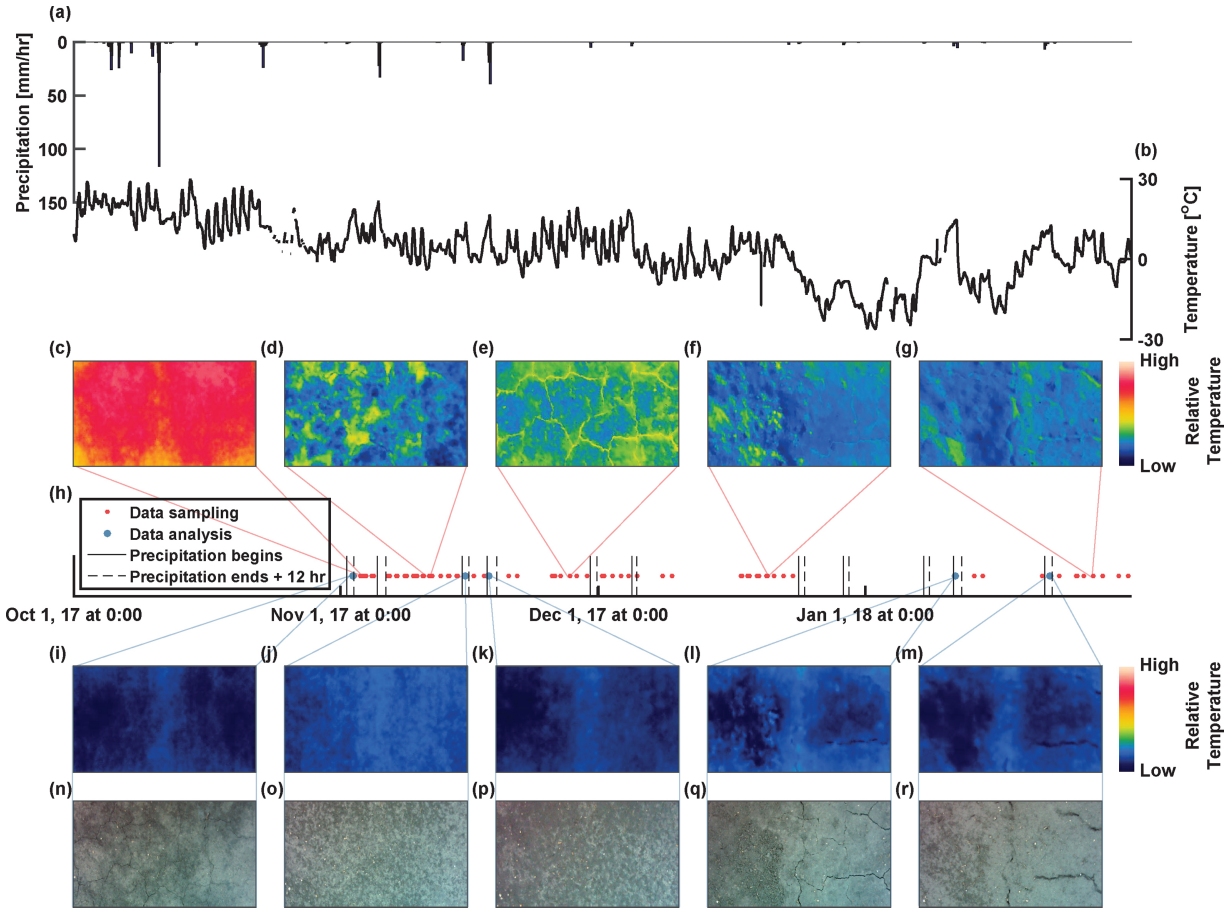


**Fig. 3.** (a) Precipitation. (b) Air temperature. After a month of transient period associated with disturbed soil conditions, thermal images were taken from November 1, 2017, to January 31, 2018, a few of which are shown in (c) to (g) for example. However, all of the thermal images taken do not provide noticeable features to detect a subsurface tile drain pipe. Therefore, (h) we chose thermal images between the beginning of precipitation (solid black line) and 12 h after the end of precipitation (dashed black line), which are shown in the blue circle and (i) to (m). The corresponding optical images are also presented in (n) to (r). (For interpretation of the references to color in this figure legend, the reader is referred to the web version of this article.)

where $T(m, n)$ is the raw thermal image and $(k, l)$ is the size of the window, $W$. The pixel values of $T(m, n)$ is replaced by the median value of the neighborhood in $W$. Here, both $k$ and $l$ were set to be 20. In the next step, thresholding was applied to the denoised image by assigning zero intensity to the pixels that had intensities lower than 80% percentile ($T_{0.8}$) of $T_{med}(m, n)$ shown as:

$$T_{TH} = \begin{cases} T_{med}(m, n) & \text{if } T_{med}(m, n) \geq T_{0.8} \\ 0 & \text{otherwise.} \end{cases} \quad (2)$$

This thresholding operation was performed based on the spatial distribution of soil heat capacity that relatively low soil moisture conditions in the areas near tile drain pipes lead to higher temperature than the other areas. Once thresholding was complete, locally separated entities in $T_{TH}$ were detected and suppressed. This processing was due to the structure of subsurface drainage systems that have geometrically linear and connected features. Next, the location of the tile was estimated through local peak detection. In this step, the processed image was subdivided into six-row images. Then, pixel values were summed up in the vertical axis within a row image so that a 1-D summation signal is obtained. The centroid of each 1-D signal was then obtained and it was mapped at the center of each subdivided row image. Linear regression was performed using the four center points to obtain a fitted line that represents the location of a tile pipe. Finally, the detected tile location (the fit line) was mapped on the optical image representing the area captured by the original raw thermal image.

## 3. Results

### 3.1. Thermal image selection

To ensure the distinctive spatial patterns of soil moisture induced by tile drainage systems (Fig. 1a), as shown in Fig. 3a we have obtained precipitation from an adjacent weather station (Latitude: 40.03 and Longitude: −88.27) from Weather Underground (https://www.wunderground.com), 10 km away from the location of the experimental device deployed. For the purpose of comparison between surface soil and air temperatures, we also show the latter in Fig. 3b.

We find that the optimum thermal image acquisition time that maximizes the contrast between the regions close to and distant from subsurface drainage pipe in thermal images is within 12 h after 2.54 mm of precipitation on the test sample (Fig. 3c to m). The threshold of 2.54 mm is determined based on previous studies (e.g. McCabe et al. (2010) and Nakano et al. (2011)), which is often used to categorize a day as dry. On the other hand, there are no strong relationships between soil and atmospheric temperatures, confirming our hypothesis that the surface soil temperature driven by tile drainage outweighs that redistributed by the thermal convection. Optical images (Fig. 3n to r) taken at the same time as the selected thermal images do

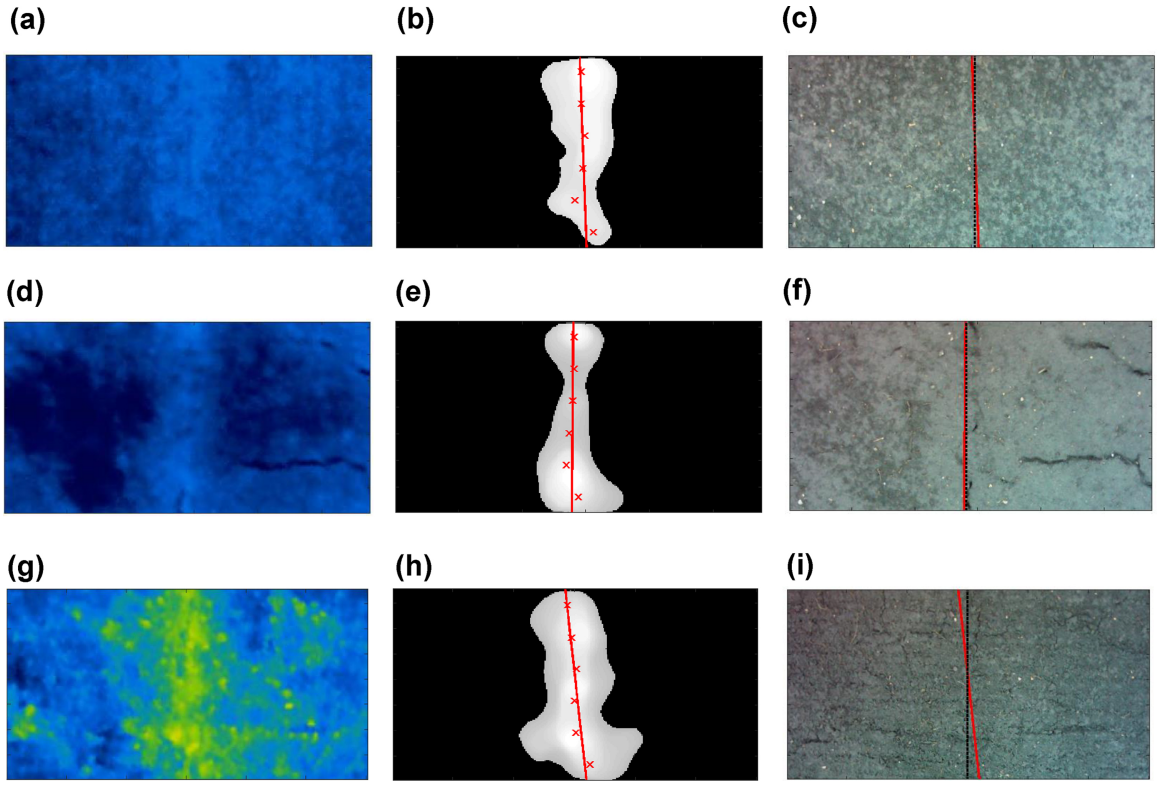


**Fig. 4.** Detection results of subsurface tile drainage system using the proposed method: (a, d and g) raw thermal images, (b, e, and h) processed images with detected tile locations and (c, f and i) optical images with mapped tile locations. The marker 'x' in the processed images represents the local peak location within a sub-divided raw image. The black dotted lines in the optical images are the locations of the subsurface drainage pipe.

not show any detectable feature linked to tile drain although identifiable cracks in the soil can be seen. This observation demonstrates that the use of thermal images has potential to provide a better prediction of subsurface tile drain systems than that of optical images. However, it is still difficult to clearly delineate subsurface tile drains with raw thermal images, thereby requiring image processing.

### 3.2. Identifying tile drainage systems

The experimental results to identify the subsurface tile drainage system using the proposed method illustrated in Fig. 2 are shown in Fig. 4. Raw thermal images obtained before introducing artificial tillage in the experimental setup are shown in Fig. 4(a) and (d). These thermal images are those shown in Fig. 3(j) and (m), respectively. Relatively high-temperature distribution is observed above the tile location (the center line of the image plane). However, the contrast between the region close to and distant from subsurface tile is not clear in the raw thermal images. The processed images using the proposed method are shown in Fig. 4(b) and (e), where the detected tile locations are also overlaid. It is seen that the tile locations are clearly visualized but not in the raw thermal images. Finally, the detected tile locations are mapped on optical images as shown in Fig. 4(c) and (f). For clear comparison, the location of the subsurface drainage pipe is indicated as black dotted lines. The tile locations are well identified by the tile-indicating line obtained by the proposed method. Note that without the mapped tile-indicating line there is no clue to identify the location of the subsurface tile in the optical images. The final mapped images demonstrate the potential of the proposed thermal image-based approach and its superior tile detectability over conventional optical image-based approaches. See more results in Fig. A.1 in Appendix.

### 3.3. Tillage effect

In order to ensure that the detection algorithm is applicable in field conditions, the effect of tillage on thermal variability needs to be accounted for. To address this, we created artificial tillage in the experimental setup to a depth of 0.6 cm, separated 2 cm apart, which was downscaled based on the experimental setup and historical tillage practices in the Midwestern United States (Baker, 2011) (Fig. 4(i)). i.e., the dominant surface noise in tile-drained agricultural areas can be expressed and evaluated to simultaneously maximize the reliability of the thermal image processing algorism developed in this study. The raw thermal, processed, and final optical images that correspond to the timeline after introducing tillage are shown in Fig. 4(g), (h) and (i), respectively. In the raw thermal image shown in Fig. 4(g), the location of the subsurface tile is intuitively identified by the contrast between the region close to and distant from the tile drain. Also, the effect of introducing tillage is negligible in the thermal image, implying that the proposed thermal image-based approach is less likely to mislead a tillage as a subsurface tile drainage pipe. In addition, the distinction between the regions with and without tile is much clearer in the processed image shown in Fig. 4(h). Finally, the detected tile location is mapped onto the optical image in Fig. 4(i). Similar to the results obtained before the tillage introduction, the location of the subsurface tile drain pipe is clearly detected even with tillage-induced multiple surface line features.

## 4. Discussion and conclusions

The surface temperature at a certain spatial point is governed by soil moisture that plays a dominant role in affecting soil heat capacity (e.g. Campbell and Norman (1998)). Therefore, the magnitude of the spatial distribution of soil heat capacity, created by subsurface water table gradients toward a drainage tile after precipitation events, should be highly influential in determining surface soil temperature. Based on this theoretical framework, in this study, we have explored and established the feasibility of using thermal images to identify subsurface tile drains rather than optical images in the downscaled experiment.

Detecting subsurface tile drainage pipes has been mostly explored using widely available optical aerial images (Verma and Cooke, 1996; Northcott et al., 2000; Varner et al., 2002; Naz and Bowling, 2008). However, this analytical approach has not provided a clear tile delineation due to surface features, such as tillage and topographic depressions (Naz and Bowling, 2008). A recent study by Allred et al. (2018) noted that surveys carried out by a drone with thermal infrared sensors could provide adequate representation of tile delineation. The proposed approach showed consistent results with those shown in Allred et al. (2018): the superior performance of thermal images over optical images in subsurface tile detection. In addition, based on the experimental results, the following conclusions are drawn: (1) there is an optimal time for thermal image acquisition that maximizes the contrast between regions close to and distant from subsurface drainage tile systems, (2) thermal images provide higher contrast between the regions close to and distant from subsurface drainage tile systems than optical images do, and (3) the proposed thermal image processing approach successfully detects and localizes subsurface drainage pipes.

Admittedly, designing a downscaled experiment that can accurately represent a large-scale experiment is often challenging. To a certain degree, the results obtained and methods presented in this study may be limiting and have unexpected flaws that may be discovered when they are deployed into an actual scale. However, given the experimental conditions and theory-based approaches, the feasibility of the use of thermal images for identifying subsurface tile drain pipes is proved by the experimental results. Therefore, this study has potential to provide an effective and promising analytical tool that can be used to precisely locate subsurface tile drain systems over a large area.

## Acknowledgement

We thank Insun Park for discussions that led to the implementation of this study and her zealous help in improving the manuscript. This work was supported by National Science Foundation (NSF) Grants ACI 1261582, EAR 1331906, and EAR 1417444, and EAR 1748573. All of the numerical information in the figures is produced by solving the equations in the paper. The precipitation and atmospheric temperature data used in this study are obtained from Weather Underground (https://www.wunderground.com).

## Appendix A

Additional experimental results to identify the subsurface tile drainage system using the proposed method are shown in Fig. A.1. Raw thermal images shown in Fig. A.1(a), (d) and (g) are those shown in Fig. 3(j), (l) (m), respectively. Similar to the experimental results shown in Fig. 4, the tile locations are well identified as seen in the processed images (Fig. A.1(b), (e) and (h)) and the optical images with mapped tile locations (Fig. A.1(c), (f) and (i)).

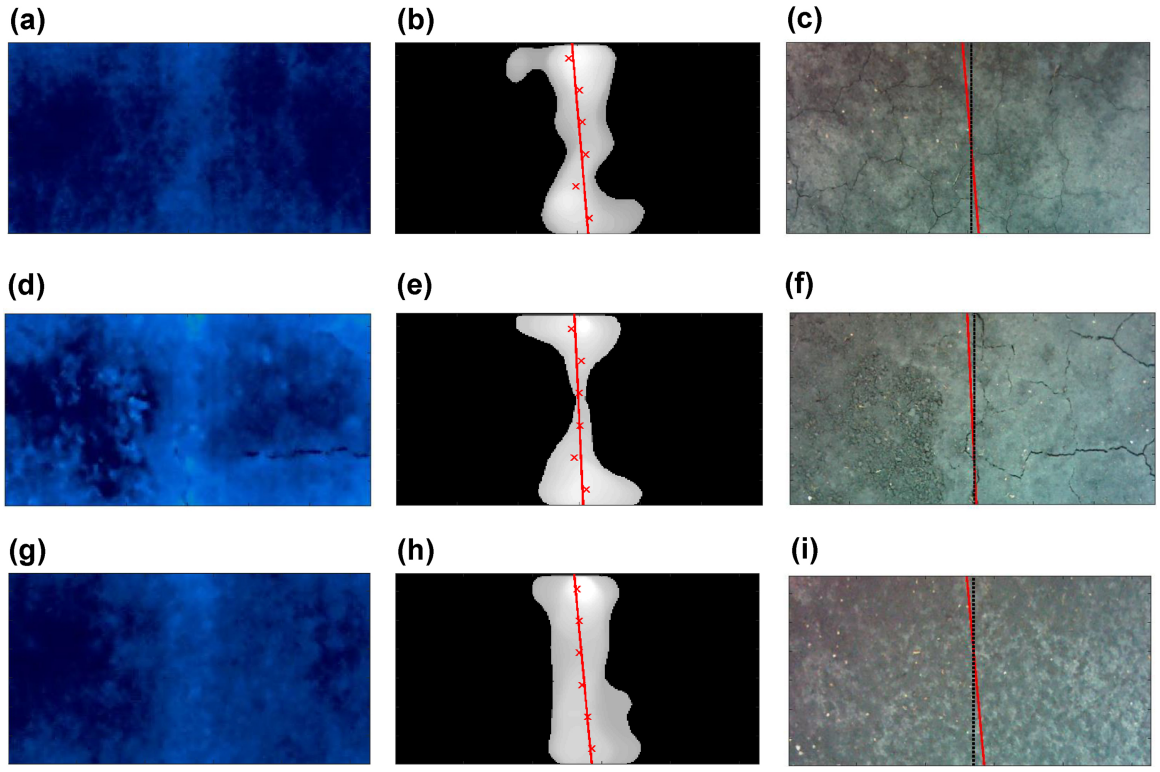


**Fig. A.1.** Additional detection results of subsurface tile drainage system: (a, d and g) raw thermal images, (b, e, and h) processed images with detected tile locations, and (c, f and i) optical images with mapped tile locations. The marker 'x' in the processed images represents the local peak location within a sub-divided raw image. The black dotted lines in the optical images are the locations of the subsurface drainage pipe.

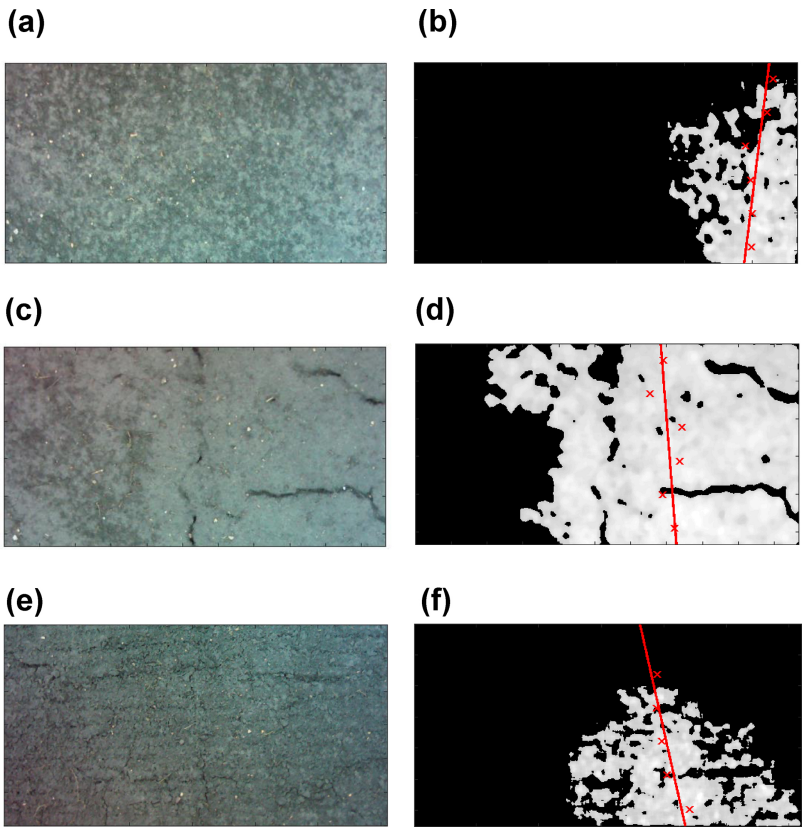


**Fig. A.2.** Failed tile detection results using the optical images and the proposed image processing approach: (a, c, e) the raw optical images corresponding to Fig. 4(c), (f) and (i), and (b, d, f) the processed images using the proposed image processing approach.

Raw optical images corresponding to Fig. 4(c), (f) and (i) and their processed images are shown in Fig. A.2. The same image processing illustrated in Fig. 2 was applied to the optical images. As seen in Fig. A.2(a), (c) and (e), raw optical images do not show clear intensity contrast between the region with and without a subsurface tile, while raw thermal images do in Fig. 4(a), (d) and (g). Fig. A.2(b), (d) and (f) show that the processed optical images fail to detect the subsurface tile. These results verify the superior performance of thermal images over optical images on subsurface tile detection.

## References


Acharya, T., Ray, A.K., 2005. Image Processing Principles and Applications. Wiley & Sons.

Allred, B., Eash, N., Freeland, R., Martinez, L., Wishart, D., 2018. Effective and efficient agricultural drainage pipe mapping with UAS thermal infrared imagery: a case study. Agric. Water Manag. 197, 132–137. https://doi.org/10.1016/j.agwat.2017.11.011.

Baker, N., 2011. Tillage practices in the conterminous United States, 1989–2004: datasets aggregated by watershed. U.S. Geological Survey Data Series, vol. 573 USGS, Reston, VA.

Campbell, G.S., Norman, J.M., 1998. Introduction to Environmental Biophysics, 2nd ed. Springer, New York.

Cannell, R.Q., Gales, K., Snaydon, R.W., Suhail, B.A., 1979. Effects of short-term waterlogging on the growth and yield of peas (Isum-Sativum). Ann. Appl. Biol. 93, 327–335. https://doi.org/10.1111/j.1744-7348.1979.tb06549.x.

Carsel, R.F., Parrish, R.S., 1988. Developing joint probability distributions of soil water retention characteristics. Water Resour. Res. 24, 755–769. https://doi.org/10.1029/WR024i005p00755.

Dinnes, D.L., Karlen, D.L., Jaynes, D.B., Kaspar, T.C., Hatfield, J.L., Colvin, T.S., Cambardella, C.A., 2002. Review and interpretation: nitrogen management strategies to reduce nitrate leaching in tile-drained midwestern soils. Agron. J. 153, 153–171.

Du, B., Arnold, J.G., Saleh, A., Jaynes, D.B., 2005. Development and application of swat to landscapes with tiles and potholes. Trans. ASAE 48 (3), 1121–1133. http://handle.nal.usda.gov/10113/43595.

Fausey, N.R., 2005. Drainage management for humid regions. Int. Agric. Eng. J. 14, 209–214.

Fausey, N.R., Brown, L.C., Belcher, H.W., Kanwar, R.S., 1995. Drainage and water quality in great lakes and cornbelt states. J. Irrig. Drain. Eng. 121, 283–288. https://doi.org/10.1061/(ASCE)0733-9437(1995)121:4(283.

Fraser, H., Fleming, R., 2001. Environmental Benefits of the Tile Drainage. Technical Report. Ridgetown College, University of Guelph.

Helmers, M., Pederson, C., Craft, K., Schott, L., 2017. Impact of drainage water management on crop yield, drainage volume, and nitrate loss. Farm Progress Reports 2016, ISRF16-34. https://doi.org/10.31274/farmprogressreports-180814-1708.

Potential water quality impact of drainage water management in the Midwest USA. In: Jaynes, D., Thorp, K.R., James, D.E. (Eds.), Proceedings of the 9th International Drainage Symposium held jointly with CIGR and CSBE/SCGAB. June 13–16, 2010, Quebec City, Canada.

Kornecki, T.S., Fouss, J.L., 2001. Quantifying soil trafficability improvements provided by subsurface drainage for field crop operations in Louisiana. Appl. Eng. Agric. 17, 777–781. https://doi.org/10.13031/2013.6846.

Lal, R., Taylor, G.S., 1970. Drainage and nutrient effects in a field lysimeter study. 2. Mineral uptake by corn. Soil Sci. Soc. Am. Proc. 34, 245–248. https://doi.org/10.2136/sssaj1970.03615995003400020020x.

Li, H., Sivapalan, M., Tian, F., Liu, D., 2010. Water and nutrient balances in a large tile-drained agricultural catchment: a distributed modeling study. Hydrol. Earth Syst. Sci. 14, 2259–2275. https://doi.org/10.5194/hess-14-2259-2010.

McCabe, G.J., Legates, D.R., Lins, H.F., 2010. Variability and trends in dry day frequency and dry event length in the southwestern United States. J. Geophys. Res 115, D07108. https://doi.org/10.1029/2009JD012866.

Nakano, M., Kanada, S., Kato, T., Kurihara, K., 2011. Monthly maximum number of consecutive dry days in Japan and its re-producibility by a 5-km-mesh cloud-system resolving regional climate mode. Hydrol. Res. Lett. 5, 11–15. https://doi.org/10.3178/hrl.5.11.

Naz, B.S., Ale, S., Bowling, L.C., 2009. Detecting subsurface drainage systems and estimating drain spacing in intensively managed agricultural landscapes. Agric. Water Manag. 96, 627–637. https://doi.org/10.1016/j.agwat.2008.10.002.

Naz, B.S., Bowling, L.C., 2008. Automated identification of tile lines from remotely sensed data. Trans. ASABE 51, 1937–1950.

Northcott, W.J., Verma, A.K., Cooke, R.A., 1996. Mapping subsurface drainage systems with color infrared aerial photographs. In: AWRA symposium on GIS and water resources. Ft. Lauderdale, FL.

Northcott, W.J., Verma, A.K., Cooke, R.A., 2000. Mapping subsurface drainage systems using remote sensing and GIS. In: ASAE Paper 002113. St. Joseph, Mich.: ASAE.
Pavelis, G., 1987. Farm Drainage in the United States: History, Status, and Prospects Miscellaneous. Publication Number 1455. U.S. Dept. of Agriculture, Economic Research Service, Washington D.C.
Radcliffe, D.E., Reid, D.K., Blomback, K., Bolster, C.H., Collick, A.S., Easton, Z.M., Francesconi, W., Fuka, D.R., Johnsson, H., King, K., Larsbo, M., Youssef, M.A., Mulkey, A.S., Nelson, N.O., Persson, K., Ramirez-Avila, J.J., Schmieder, F., Smith, D.R., 2015. Applicability of models to predict phosphorus losses in drained fields: a review. J. Environ. Qual. 44 (2), 614–628. https://doi.org/10.2134/jeq2014.05.0220.
Randall, G.W., Iragavarapu, T.K., 1995. Impact of long-term tillage systems for continuous corn on nitrate leaching to tile drainage. J. Environ. Qual. 24, 360–366. https://doi.org/10.2134/jeq1995.00472425002400020020x.
Shokri, A., Bardsley, E., 2014. Enhancement of the hooghoudt drain-spacing equation. J. Irrig. Drain. Eng. 141, 04014070. https://doi.org/10.1061/(ASCE)IR. 1943-4774.0000835.
Sugg, Z., 2007. Assessing U.S. Farm Drainage: Can GIS Lead to Better Estimates of Subsurface Drainage Extent? World Resources Institute, Washington, D.C.
Varner, B.L., Gress, T., Copenhaver, K., White, S., 2002. The Effectiveness and Economic Feasibility of Image Based Agricultural Tile Maps. Technical Report. Inst. of Tech, Champaign, IL Final Report to NASA ESAD.
Verma, A., Cooke, R., 1996. Mapping subsurface drainage systems with color infrared aerial photographs. AWRA Symposium on GIS and Water Resources.
Wang, X.Y., Wang, Y., Tian, X.H., Ma, G.H., 2011. Effects of nmurea on nitrogen runoff losses of surface water and nitrogen fertilizer efficiency in paddy field. Trans. CSAE 27, 106–111.
Wilkins, B., Woo, D.K., Michalski, G., Kumar, P., Keefer, D., Keefer, L., Fisher, M., Li, J., Hodson, T., Welp, L., Conroy, J., 2019. Quantification of Field Scale Denitrification by Stable Isotope Analysis of $NO_3$ and $H_2O$ From Tile Drain Runoff. Water Resour. Res (submitted for publication).
Woo, D.K., Kumar, P., 2019. Impacts of subsurface tile drainage on age-concentration dynamics of inorganic nitrogen in soil. Water Resour. Res. 55, 1470–1489. https://doi.org/10.1029/2019WR024139.
Wright, J., Sands, G., 2001. Planning an agricultural subsurface drainage system. University of Minnesota Extension Bulletin BU-07865-S. University of Minnesota, St. Paul, MN, USA.
Zucker, L., Brown, L., 1998. Agricultural Drainage: Water Quality Impacts and Subsurface Drainage Studies in the Midwest. Ohio State University Extension Bulletin, pp. 871.